Physics of Fluids LETTER pubs.aip.org/aip/pof

Capillary rise on rounded polygon corners of pillar and array structures

Cite as: Phys. Fluids **36**, 101701 (2024); doi: 10.1063/5.0231539
Submitted: 31 July 2024 · Accepted: 12 September 2024 ·
Published Online: 1 October 2024

Jonghyun Ha (하종현),[1] Keunhwan Park (박근환),[2,a)] and Wonjong Jung (정원종)[2,a)]

AFFILIATIONS

[1]Department of Mechanical Engineering, Ajou University, Suwon 16499, Republic of Korea
[2]Department of Mechanical, Smart, and Industrial Engineering, Gachon University, Seongnam 13120, Republic of Korea

[a)]**Authors to whom correspondence should be addressed:** kpark@gachon.ac.kr and wonjongjung@gachon.ac.kr

ABSTRACT

Capillary rise, where liquid climbs narrow spaces against gravity, plays an important role in both natural and technological processes. This study investigates capillary wetting in rounded polygon corners, a less-studied area in microfluid mechanics with significant implications for industries such as nanotextured surface cleaning, micro-soldering, food technology, and water harvesting. Through experimental analysis, we examine the relationship between capillary rise height and the geometric parameters of curvature radius and angle in rounded polygonal pillar and array structures. Our findings reveal a direct correlation where the capillary rise height increases as the radius of the corner increases, emphasizing the critical role of corner geometry in enhancing capillary action. This research not only deepens understanding of capillary behavior in complex geometries but also provides valuable insights for optimizing capillary-based applications across. By considering the influence of geometric complexity on capillarity, our study paves the way for innovative approaches in the design and development of efficient systems for fluid manipulation and control.

Capillary behavior in narrow spaces is a fundamental phenomenon observed both in nature and in various technological applications.[1–3] This intriguing phenomenon, driven by the interplay of cohesive and adhesive forces, is observed not only in practical fields in microfluid mechanics[4] but also in numerous practical applications.[5,6] In our daily lives, capillary action can be seen in the way plants transport water from their roots to their leaves, defying gravity to nourish their uppermost parts.[7–9] Similarly, the absorption of ink by paper,[10] the movement of water through a sponge,[11,12] and the functionality of everyday items like paper towels all rely on capillary principles. These simple yet essential processes highlight the capillary action in everyday surroundings.

In the industrial area, capillary action plays an important role in several advanced technologies and processes. For instance, in the cleaning of nanotextured surfaces, understanding capillary wetting can lead to the development of more efficient cleaning methods that ensure thorough removal of contaminants at the microscopic level.[13–16] In dip coating processes, which are used to apply uniform coatings to complex geometries, the capillary rise of liquids is crucial for achieving consistent and defect-free coatings.[5,17] In food technology, specifically in the chocolate coating process, capillary action is essential for evenly distributing melted chocolate over confections, ensuring a smooth and uniform finish.[18] Micro-soldering, used in the assembly of microelectronics, relies on capillary forces to draw molten solder into tiny gaps and around intricate components, ensuring reliable electrical connections.[19,20] Additionally, water harvesting technologies, especially those designed for arid regions, depend on optimizing capillary structures to maximize water collection from dew and fog.[21–23]

Despite the extensive research on capillary rise on cylindrical pillars, as shown in Fig. 1(a), the behavior of liquids in more complex shapes, such as rounded corners at polygonal pillars and array [see Figs. 1(b) and 1(c)], remains insufficiently studied to the best of our knowledge. Understanding the capillary action in these more complex shapes is important, as they are often encountered in practical applications and natural phenomena.[24,25] The analysis of capillary rise in rounded corners of polygonal pillars and pillar arrays is particularly challenging due to intricate interplay between capillary forces and geometric features, like curvature radius and corner angle. Sharp corners present additional difficulties as they are mathematically considered singular points, making theoretical analysis complex and often infeasible. In contrast, rounded corners can avoid this singularity, allowing us to provide more robust theoretical predictions. Gaining insight into these behaviors is essential for achieving more accurate predictions and optimization in various fields, including microfluidics, materials

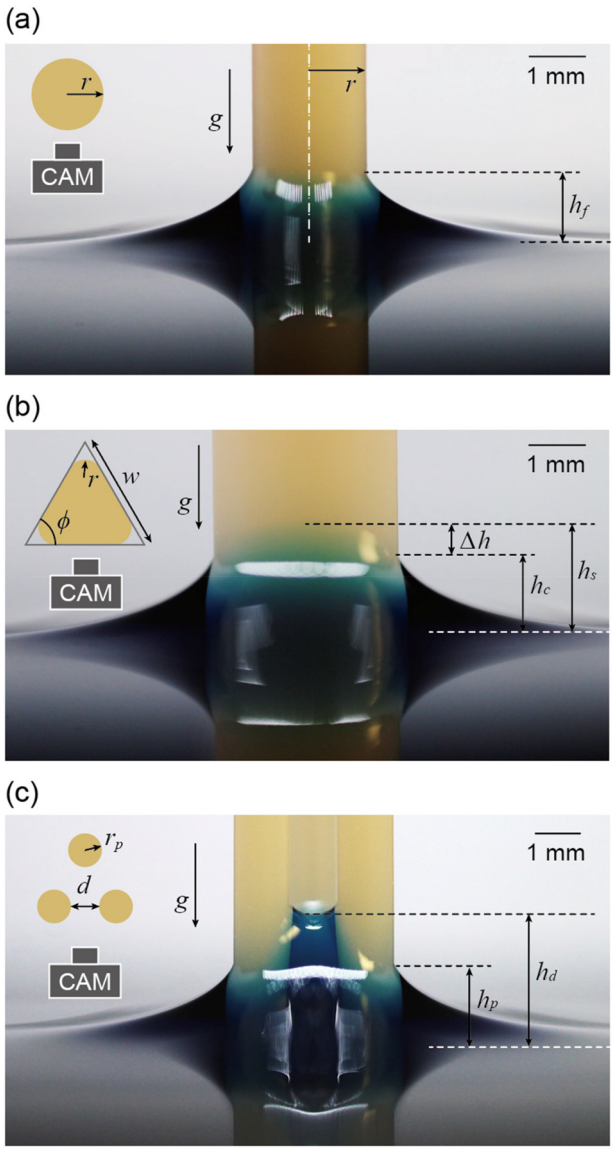

FIG. 1. Experimental images of capillary rise on rounded structures. (a) Cylindrical fiber. (b) Rounded triangular pillar. (c) Pillar array.

science, and biological systems. Through experimental analysis, the effects of geometric parameters on capillary rise can be understood, leading to the development of theoretical models that accurately predict these behaviors.

To measure the rise height at the rounded corners of polygonal pillars, we fabricate the pillars with a specified fillet radius, r, using a high-precision 3D printer (Micro cDLM, EnvisionTEC) with a z-axis resolution of approximately 1 μm. Given this high resolution, we believe that the surfaces of the pillars are sufficiently smooth, minimizing the potential impact of surface roughness on capillary rise. The smoothness of these surfaces ensures that the capillary action is primarily governed by the geometric features of the pillars, such as the corner radius and angle, rather than by microscopic irregularities. The resin material used in this 3D printing process is not hydrophilic, making it unsuitable for our capillary wetting experiments with water. To address this limitation, we treat the surfaces of the polygonal pillars with a plasma treatment machine (Zepto, Diener), thereby rendering them hydrophilic and suitable for capillary wetting experiments.

To provide a comparative analysis, we measure the contact angles on both plasma-treated and untreated surfaces. The plasma-treated surfaces exhibit a significantly reduced contact angle of approximately $16 \pm 2°$, compared to $65 \pm 7°$ on the untreated surfaces. This reduction in contact angle on the plasma-treated surfaces indicates a substantial enhancement in wettability, which is critical for efficient execution of capillary rise experiments. However, this hydrophilic effect induced by plasma treatment can diminish over time due to surface aging or contamination. The experiments are conducted over a short period, during which the enhanced hydrophilic effects of the plasma treatment are maintained. We prepare a solution of water with blue dye, which enhances the visibility of the water interface and facilitates precise measurement without altering the physical properties of the water (see Fig. 1). Upon immersing the hydrophilic polygonal pillars into the dyed water, capillary action causes the water to rise against gravity until it reaches an equilibrium height. For the pillar array, we experiment a triangular array, as shown in Fig. 1(c).

We optically measure the capillary rise height on the polygonal pillar. We note the rise height at two distinct locations: along the plane of the polygonal faces, h_s, and at the rounded corners, h_c, as illustrated in Fig. 1(b). For the pillar array [see Fig. 1(c)], we measure the rise height at the pillars, h_p, and in the spacing between pillars, h_d. Our measurements indicate that $h_c < h_s$ and $h_p < h_d$, which is attributed to the geometric effects of the corners. These observations show the influence of corner geometry on capillary rise and provide essential data for validating our theoretical models.

The capillary rise height on a cylindrical fiber can be theoretically described by the equation $h_f \sim r\ln(l_c/r)$, where $l_c = [\gamma/(\rho g)]^{1/2}$ represents the capillary length, γ is the surface tension, ρ is the liquid density, g is the acceleration due to gravity, and r is the radius of the fiber.[26] The capillary length, l_c, typically represents the radius of curvature of the liquid meniscus, as illustrated in Fig. 2(a). The theoretical expression for the capillary rise height, h_f, is applicable under the condition that the fiber radius is much smaller than the capillary length, specifically $l_c \gg r$. Under these circumstances, the logarithmic dependence on the radius provides an accurate prediction of the rise height. However, this model fails when applied to the rounded corners of polygonal pillars and array configuration. The observed rise height at the corners, h_c and h_p, exceeds the predicted height h_f derived from the cylindrical fiber model. This discrepancy indicates that the cylindrical model does not account for the geometric complexities introduced by the polygonal shape, array, and rounded corners. Therefore, a modified theoretical model is required to accurately describe the capillary rise in these more complex geometries, taking into consideration the effects of corner curvature and angular variations. To accurately predict the capillary rise on polygonal structures, we assume that an additional force is exerted at the corners, leading to an increased capillary rise height beyond the theoretical h_f. We first investigate the rise height on individual polygonal pillars, then extend our analysis to triangular pillar arrays.

Based on the assumption of the additional force, we can express the rise height at the corner of the polygonal pillar as h_c,

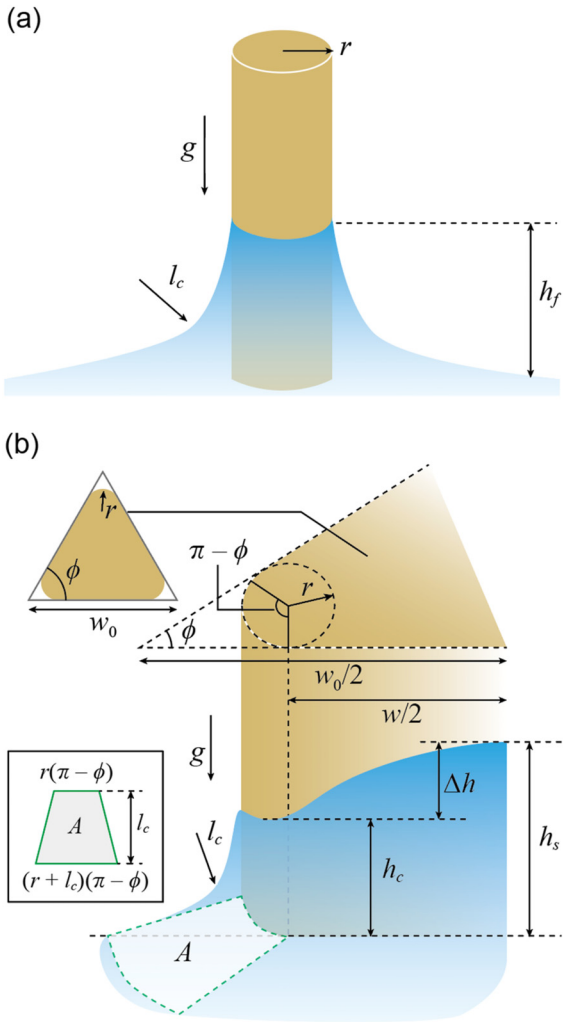

FIG. 2. Model schematics of capillary rise height. (a) Cylindrical fiber. (b) Rounded triangular pillar. The inset indicates the projected area.

$$h_c \sim h_f + \alpha_c \Delta h_c, \tag{1}$$

where α_c is the prefactor and Δh_c represents the increment in rise height. The prefactor, α_c, in Eq. (1) was determined through a series of calibration experiments, where capillary rise heights were measured across various geometric configurations and the data were fitted to the theoretical model. We typically express Δh_c as the equilibrium rise height by balancing the effective capillary pressure, Δp_c, against the hydrostatic pressure, $\rho g \Delta h_c$. The effective capillary pressure can be approximated as $\Delta p_c \sim F/A$, where $F \sim \gamma w$ denotes the surface force, with γ being the surface tension and w the width of the planar section. Considering geometric feature [see Fig. 2(b)], $w = w_0 - 2r\tan[(\pi - \phi)/2]$, where w_0 is the width of the polygons, r is the radius of the rounded corner, and ϕ is the angle subtended by the corner. The area A is determined by the projected area of the liquid meniscus on the rounded corner, which adopts a trapezoidal shape: $A \sim [r(\pi - \phi) + l_c]l_c$. Figure 2(b) shows capillary wetting on the rounded corner of a triangular pillar, while the inset of Fig. 2(b) illustrates the trapezoidal projected area of the liquid meniscus. By balancing the effective capillary pressure, Δp_c, and the hydrostatic pressure, $\rho g \Delta h_c$, we derive $\Delta h_c \sim l_c^2 w/A$ of Eq. (1), where $l_c = (\gamma/\rho g)^{1/2}$ is the capillary length. This theoretical framework of Eq. (1) provides a comprehensive understanding of the increased capillary rise height at the rounded corners of polygonal pillars, offering insight into the complex interplay between geometric features and capillary forces. By incorporating these considerations, fluid behavior in applications involving capillary action in complex geometries can be more accurately predicted and effectively controlled.

The theoretical equation proposed in this study, as described in Eq. (1), are validated through a series of experimental observations. We optically measure the capillary rise height on rounded polygonal pillars, as depicted in Fig. 3(a). In our experiments, we distinguish between the capillary rise height at the corners, h_c, and the planes, h_s, of the pillars. Figure 3(b) presents a detailed analysis of h_c for triangular pillars with varying corner radii, r. The inset of Fig. 3(b) provides top-view images of the rounded triangular shapes, illustrating the increase in r. The graph compares the current theoretical model for h_c (black dashed lines) with the previously established model for $h_f \sim r\ln(l_c/r)$[26] (red dashed lines).

Our experimental data reveal a significant discrepancy between h_c and h_f at smaller corner radii, which gradually diminishes as r increases. As the corner radius decreases, the relative contribution of the side surfaces becomes more pronounced, thereby increasing the effective capillary pressure at the corners. This enhanced capillary pressure leads to a higher h_c at the corners compared to h_f observed in cylindrical structures with the same radius. Notably, when r approaches the radius of the inscribed circle of the triangle (i.e., $r = 1$ mm), the rise height h_c converges with h_f ($\Delta h_c = 0$). This convergence suggests that at larger corner radii, the capillary rise behavior approximates that predicted by the simpler cylindrical fiber model.[26] The agreement between our theoretical model for h_c and the experimental results shows the robustness of our approach in capturing the nuances of capillary rise in polygonal geometries. This validation highlights the critical role of corner radius in modulating capillary rise and provides a refined framework for predicting fluid behavior in polygonal pillars with rounded corners.

At the planar sections of the pillar (denoted as w), the capillary rise height, h_s, can be expressed geometrically using a linear interpolation method as follows:

$$h_s \sim h_c + \alpha_s(1 - h_c/l_c)w, \tag{2}$$

where α_s is a prefactor determined to fit the experimental data precisely. Similar to the observations in Fig. 3(b), Fig. 3(c) shows significant discrepancy between the theoretical rise height h_f and the experimentally measured h_s. This discrepancy decreases as the corner radius r increases. Despite the simplicity of our scaling law of Eq. (2), it effectively captures the experimental data for h_s. Furthermore, we analyze the curvature, κ, at the plane sections, as depicted in Fig. 3(a), with respect to varying r. The curvature can be approximated by the expression $\kappa \sim (h_s - h_c)/w^2$. Figure 3(d) shows that the theoretically predicted κ aligns closely with the experimental results, demonstrating the accuracy of our model. Specifically, the liquid meniscus in the wider pillar tends to stabilize, forming a nearly flat interface, especially along the planar surface of the pillar. This confirms that for wider

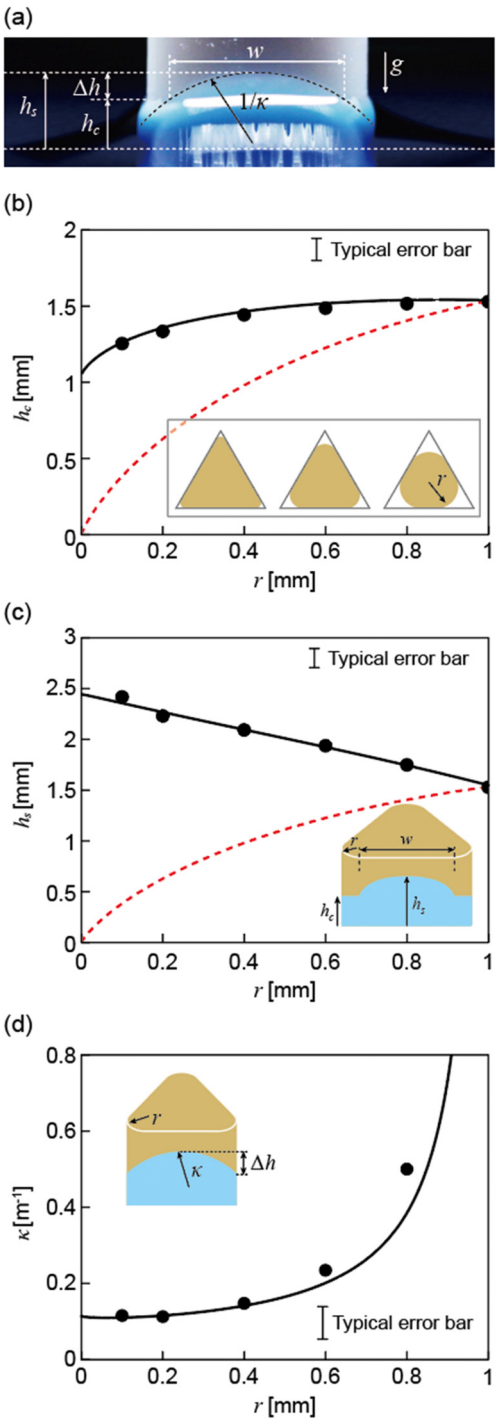

FIG. 3. Comparison between the theoretical model and experimental results. (a) Experimental measurements of capillary rise heights at the corners, h_c, and planes, h_s, of polygonal pillars. (b) Plot of h_c vs corner radius r. The black line represents the theoretical prediction from Eq. (1), while the red dashed line indicates the theoretical height, h_f. $\alpha_c = 0.3$. (c) Plot of h_s vs corner radius r. The black line corresponds to the theoretical prediction from Eq. (2). $\alpha_s = 1.3$. (d) Plot of curvature, κ, vs corner radius r. The black line shows the theoretically predicted κ.

polygonal pillars, the capillary rise is governed by the capillary length, leading to a more uniform and predictable meniscus shape.

To systematically evaluate the influence of corner angle on capillary rise, we fabricate a series of rounded polygonal pillars with corner radius fixed at $r = 0.4$ mm, ranging from triangular to octagonal shapes. Figure 4(a) illustrates the capillary wetting observed on these various polygonal pillars. We optically measure the capillary rise height at the corners, h_c, for each polygonal configuration and plotted these values against the corresponding corner angles, ϕ, as shown in Fig. 4(b). According to Eq. (1), the rise height, h_c, is a function of not only the corner radius, r, but also the corner angle, ϕ. At lower corner angles, the liquid meniscus curves more sharply, resulting in a higher projected area of the liquid meniscus at the corners, which decreases h_c. Conversely, at higher corner angles, the area is less pronounced, leading to an increased h_c. Thus, both the corner radius and angle significantly influence the rise height.

The theoretical predictions for h_c across different corner angles demonstrate a strong correlation with the experimental data, confirming the validity of our model. Specifically, for lower corner angles (e.g., in triangular and square pillars), the theoretical prediction agrees well with the experimental h_c. However, at higher corner angles (e.g., hexagonal and octagonal pillars), we observe a slight discrepancy between the model predictions and the experimental results. This divergence can be attributed to the fact that the size of pillars with larger corner

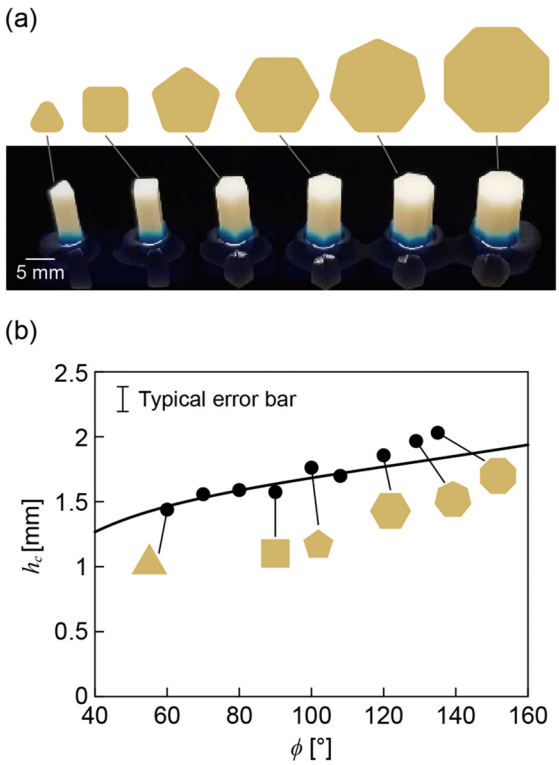

FIG. 4. Various polygonal pillars. (a) Experimental images showing capillary wetting on rounded polygonal pillars with shapes ranging from triangles to octagons. (b) Plot of h_c vs corner angle ϕ. The black line represents the theoretical prediction from Eq. (1).

angles extends beyond the typical capillary regime, thereby introducing additional factors that are not fully captured by the current theoretical model. These factors may include variations in surface tension effects and deviations from ideal geometric assumptions.

We now move on to the capillary wetting behavior in a triangular pillar array. In addition to individual triangle-shaped pillars, we fabricate arrays of three pillars arranged in a triangular configuration and conduct capillary rise experiments varying the pillar radius, r_p, and spacing, d. We measure the rise height at the pillars, h_p, and in the spacing between pillars, h_d, as shown in Fig. 1(c). Our experiments reveal that both h_p and h_d increase with increasing r, but they decrease inversely with increasing d.

Figure 5(a) illustrates the schematic model for capillary rise on triangular pillars. For the rise height in the spacing, h_d, the driving force for the capillary rise is induced by the surface tension at the pillar, described as $F_c \sim \gamma r$. The resisting force due to gravity can be expressed as $F_w \sim \rho g d l_c h_d$, considering the liquid volume, $d l_c h_d$, surrounding the pillars. Balancing these forces leads to

$$h_d \sim \alpha_d r l_c / d, \tag{3}$$

where α_d is a prefactor determined to precisely fit the experimental data. We plot Eq. (3) with respect to d and compare it with the experimental results for various r. Figure 5(b) demonstrates good agreement between the theoretical model and the experimental data for different values of r and d.

For the rise height at the pillars, h_p, we recall the additional height, similar to the expression in Eq. (1),

$$h_p \sim h_f + \alpha_p \Delta h_p, \tag{4}$$

where α_p is a prefactor and Δh_p is an additional rise height of the pillar array. The capillary pressure between the spacings, γ/d, effectively raises the liquid column to a height greater than h_f. This effective pressure balances with the additional hydrostatic pressure $\rho g \Delta h_p$, leading to $\Delta h_p \sim \gamma/(\rho g d)$. Our theoretical model, described by Eq. (4), is corroborated by the experimental results [see Fig. 5(c)]. Please note that h_p converges to h_f as d increases since the effective capillary pressure diminishes with larger spacing, reducing its influence on the liquid column rise. This physical explanation qualitatively accounts for capillary wetting on cylindrical fibers and interactions within complex structures such as polygonal shapes and arrays, showing parallels between Eqs. (1) and (4).

We conduct additional experiments to further investigate the dynamics of capillary rise over time, specifically focusing on the rise dynamics at the corners and flat faces of the rounded polygonal pillars. As shown in Fig. 6, our experimental results demonstrate that the capillary rise initially exhibits a time dependence proportional to $t^{1/2}$, consistent with the Lucas–Washburn law.[27] This indicates that in the early stages, the liquid ascends along the surface of the pillars at a rate proportional to the square root of time. As the liquid approaches the equilibrium height, the rate of rise decreases, and the capillary rise height gradually approaches the equilibrium value. Our experimental findings provide clear evidence that the capillary rise in these structures conforms to the expected behavior described by the Lucas–Washburn law.

In this study, we investigated the capillary wetting behavior in rounded polygon corners and triangular pillar arrays. Through experimental analysis, we explored the relationship between capillary rise height, curvature radius, and corner angle in polygonal pillars. Our

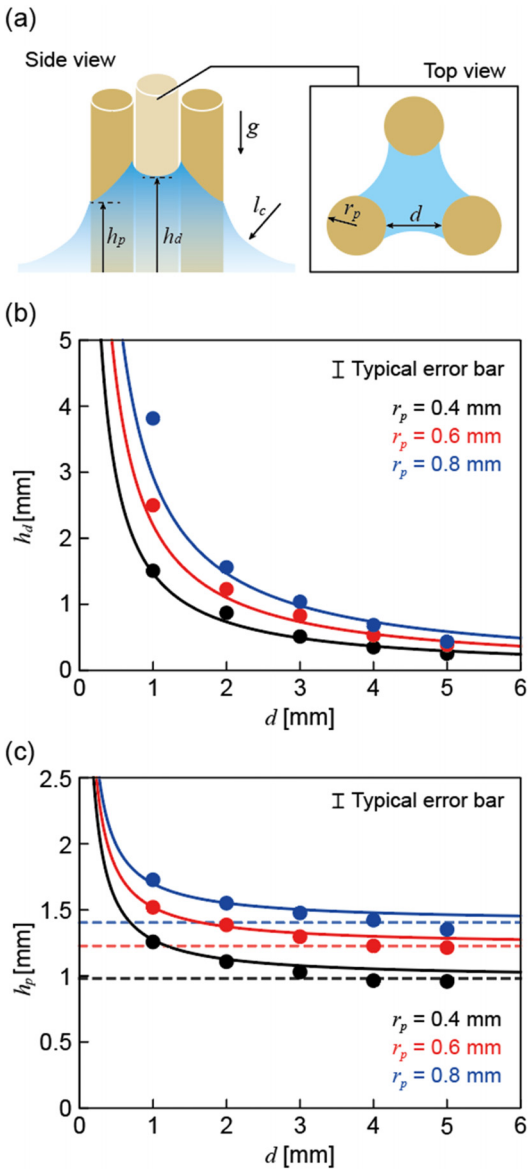

FIG. 5. Capillary wetting on triangular pillar array. (a) Schematic representation of the modeling approach, shown in top and side views. The curvature of the side meniscus is typically expressed as the capillary length, l_c. (b) Plot of h_d vs d. The solid lines represent the theoretical model of Eq. (3). $\alpha_d = 1.5$. (c) Plot of h_p vs d. The solid lines correspond to the theoretical model from Eq. (4), while the dashed lines indicate the theoretical height h_f. $\alpha_p = 0.04$.

findings reveal that h_c increases as r and ϕ increase, emphasizing the critical role of corner geometry in capillary action. We extended our investigation to triangular pillar arrays, examining how variations in pillar radius and spacing influence capillary rise. The results demonstrated that both h_p and h_d are positively correlated with pillar radius and inversely proportional to the spacing between pillars.

The model developed in this study, based on scaling analysis, is intended to capture the general trend of capillary rise at polygon

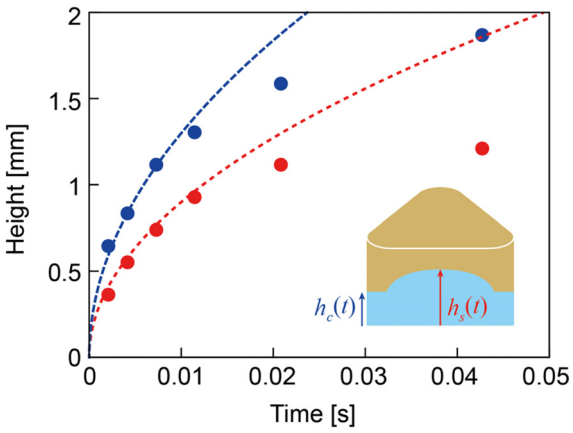

FIG. 6. Dynamics of capillary rise on rounded triangular pillars with $r = 0.2$ mm. The blue and red curves represent the dynamics of h_c and h_s, respectively. The dashed lines indicate the $t^{1/2}$ dependence, with curve fitting parameters of 11 for h_c and 16 for h_s.

corners rather than to provide precise predictions through detailed numerical analysis. The scaling approach simplifies the complex interactions between capillary forces and geometric features, allowing for general insights into how these forces drive liquid rise along the corners of polygonal structures. While this model effectively captures the overall trend of capillary rise, the incorporation of prefactors is necessary to refine the comparisons with experimental results, as the scaling analysis alone does not account for all the nuances of real-world geometries. Our observations indicate that the prediction model with a constant $\alpha_c = 0.3$ shows good agreement with experimental data across a range of corner radii, as illustrated in Fig. 3(b). Additionally, the model performs well for different corner angles, maintaining consistency even when α_c is held constant at 0.3. This suggests that the chosen prefactor effectively captures the essential physics governing capillary rise in these complex geometries, reinforcing the robustness of the simplified model under varying conditions.

The agreement between our theoretical predictions and experimental observations across different geometrical parameters validates the robustness of the theoretical model. Our findings highlight the critical influence of corner radius on capillary rise heights and curvature, providing physical insights for predicting capillary behavior in polygonal structures. We expect our study to contribute to the broader understanding of capillary phenomena in complex geometries, offering valuable perspectives for future technological advancements in various industries. As the corner radii of polygonal pillars increase, the theoretical model proves especially useful in the design of wicking materials used in heat pipes and other thermal management systems. The temperature of the liquid and its environment significantly affects capillary rise in rounded polygonal pillars due to its impact on surface tension. As the temperature increases, surface tension decreases, resulting in a lower capillary rise height, while lower temperatures increase surface tension, leading to a higher rise. These temperature-dependent variations are critical for applications requiring precise control of liquid movement and must be considered in design and operational processes.

ACKNOWLEDGMENTS

This work was supported by the National Research Foundation of Korea (NRF) grant funded by the Korea government (No. RS-2024-00341444) and the Gachon University research fund of 2019 (No. GCU-2019-0800).

AUTHOR DECLARATIONS

Conflict of Interest

The authors have no conflicts to disclose.

Author Contributions

Jonghyun Ha: Conceptualization (equal); Funding acquisition (equal); Supervision (equal); Writing – original draft (equal). **Keunhwan Park:** Resources (equal); Writing – original draft (equal); Writing – review & editing (equal). **Wonjong Jung:** Supervision (equal); Writing – original draft (equal); Writing – review & editing (equal).

DATA AVAILABILITY

The data that support the findings of this study are available from the corresponding author upon reasonable request.

REFERENCES

[1]J. Bico and D. Quéré, "Rise of liquids and bubbles in angular capillary tubes," J. Colloid Interface Sci. **247**, 162–166 (2002).
[2]M. Stange, M. E. Dreyer, and H. J. Rath, "Capillary driven flow in circular cylindrical tubes," Phys. Fluids **15**, 2587–2601 (2003).
[3]J. Ha, Y. S. Kim, R. Siu, and S. Tawfick, "Dynamic pattern selection in polymorphic elastocapillarity," Soft Matter **18**, 262–271 (2022).
[4]J. Ha and H. Y. Kim, "Capillarity in soft porous solids," Annu. Rev. Fluid Mech. **52**, 263–284 (2020).
[5]A. Sauret, A. Gans, B. Colnet, G. Saingier, M. Z. Bazant, and E. Dressaire, "Capillary filtering of particles during dip coating," Phys. Rev. Fluids **4**, 054303 (2019).
[6]D. Brutin and V. Starov, "Recent advances in droplet wetting and evaporation," Chem. Soc. Rev. **47**, 558–585 (2018).
[7]B. Shin, S. Jung, M. Choi, K. Park, and H. Y. Kim, "Plant-inspired soft actuators powered by water," MRS Bull. **49**, 159–172 (2024).
[8]K. Park, J. Knoblauch, K. Oparka, and K. H. Jensen, "Controlling intercellular flow through mechanosensitive plasmodesmata nanopores," Nat. Commun. **10**, 3564 (2019).
[9]A. D. Stroock, V. V. Pagay, M. A. Zwieniecki, and N. M. Holbrook, "The physicochemical hydrodynamics of vascular plants," Annu. Rev. Fluid Mech. **46**, 615–642 (2014).
[10]J. Kim, M. W. Moon, K. R. Lee, L. Mahadevan, and H. Y. Kim, "Hydrodynamics of writing with ink," Phys. Rev. Lett. **107**, 264501 (2011).
[11]J. Ha, J. Kim, Y. Jung, G. Yun, D. N. Kim, and H. Y. Kim, "Poro-elasto-capillary wicking of cellulose sponges," Sci. Adv. **4**, eaao7051 (2018).
[12]J. I. Siddique, D. M. Anderson, and A. Bondarev, "Capillary rise of a liquid into a deformable porous material," Phys. Fluids **21**, 013106 (2009).
[13]B. Liang, I. M. Zarikos, W. B. Bartels, S. M. Hassanizadeh, and A. Clarens, "Effect of nanoscale surface textures on multiphase flow dynamics in capillaries," Langmuir **35**, 7322–7331 (2019).
[14]T. Heckenthaler, S. Sadhujan, Y. Morgenstern, P. Natarajan, M. Bashouti, and Y. Kaufman, "Self-cleaning mechanism: Why nanotexture and hydrophobicity matter," Langmuir **35**, 15526–15534 (2019).
[15]Y. Li, J. Lin, M. Xi, J. Wu, and J. Long, "Effects of surface nanotexturing on the wickability of microtextured metal surfaces," J. Colloid Interface Sci. **638**, 788–800 (2023).
[16]Y. A. Lee, C. Y. Oh, S. J. Park, P. J. Yoo, and M. W. Moon, "Superhydrophilic conformal polydopamine coating on nanostructured surface formed by capillary-induced solution infusion," Surf. Interfaces **48**, 104344 (2024).

[17]B. M. Dincau, M. Z. Bazant, E. Dressaire, and A. Sauret, "Capillary sorting of particles by dip coating," Phys. Rev. Appl. **12**, 011001 (2019).
[18]S. Wichchukit, M. J. McCarthy, and K. L. McCarthy, "Flow behavior of milk chocolate melt and the application to coating flow," J. Food Sci. **70**, E165–E171 (2005).
[19]J. Gu, W. T. Pike, and W. J. Karl, "A novel capillary-effect-based solder pump structure and its potential application for through-wafer interconnection," J. Micromech. Microeng. **19**, 074005 (2009).
[20]M. Mastrangeli, W. Ruythooren, J. P. Celis, and C. Van Hoof, "Challenges for capillary self-assembly of microsystems," IEEE Trans. Compon., Packag., Manuf. Technol. **1**, 133–149 (2010).
[21]X. Li, G. Zhang, C. Wang, L. He, Y. Xu, R. Ma, and W. Yao, "Water harvesting from soils by light-to-heat induced evaporation and capillary water migration," Appl. Therm. Eng. **175**, 115417 (2020).
[22]S. Zhang, J. Huang, Z. Chen, and Y. Lai, "Bioinspired special wettability surfaces: From fundamental research to water harvesting applications," Small **13**, 1602992 (2017).
[23]A. Lee, M. W. Moon, H. Lim, W. D. Kim, and H. Y. Kim, "Water harvest via dewing," Langmuir **28**, 10183–10191 (2012).
[24]G. Mason and N. R. Morrow, "Capillary behavior of a perfectly wetting liquid in irregular triangular tubes," J. Colloid Interface Sci. **141**, 262–274 (1991).
[25]S. Herminghaus, M. Brinkmann, and R. Seemann, "Wetting and dewetting of complex surface geometries," Annu. Rev. Mater. Res. **38**, 101–121 (2008).
[26]D. Quéré and J. M. Di Meglio, "The meniscus on a fibre," Adv. Colloid Interface Sci. **48**, 141–150 (1994).
[27]R. Lucas, "Ueber das Zeitgesetz des kapillaren Aufstiegs von Flüssigkeiten," Kolloid Z. **23**, 15–22 (1918).